






## Thermal Effects in Lubrication of Asymmetric Rollers Using Roelands Viscosity-Pressure Equation Including Convection

Swetha Lanka<sup>1,2</sup>, Venkata Subrahmanyam Sajja<sup>1\*</sup>, Dhaneshwar Prasad<sup>3</sup>

<sup>1</sup> Department of Engineering Mathematics, Koneru Lakshmaiah Education Foundation, Guntur 522502, Andhra Pradesh, India

<sup>2</sup> Department of Mathematics, Sir C R Reddy College of Engineering, Eluru 534007, Andhra Pradesh, India

<sup>3</sup> Formerly Department of Mathematics, Kanchi Mamunivar Government Institute for Post Graduate Studies and Research, Puducherry 605008, India

Corresponding Author Email: [subrahmanyam@kluniversity.in](mailto:subrahmanyam@kluniversity.in)

<https://doi.org/10.18280/ijht.410324>

### ABSTRACT

**Received:** 1 February 2023

**Accepted:** 14 June 2023

#### Keywords:

*hydrodynamic lubrication, non-Newtonian, Bingham plastic, incompressible, viscosity*

In order to study fluid film bearing systematically, the determination of optimal parameters is vital. A theoretical analysis of lubrication of asymmetric roller bearings with rolling and sliding motion lubricated by a non-Newtonian incompressible Bingham plastic fluid is presented with cavitation boundary conditions for heavily loaded rigid system. The Roeland lubricant viscosity is considered to vary with pressure and mean film temperature. The fluid flow governing equations such as equation of motion with continuity and momentum energy equations are first reduced to ordinary differential equations applying appropriate approximation and then solved numerically using MATLAB. This article discusses and elaborates on the various important characteristics of bearings including velocity, pressure, viscosity, mean temperature, load and traction. Graphs and table are introduced for Newtonian and non-Newtonian fluids to make clarity of this work. The results are found qualitatively in good agreement with those obtained by prior researchers.

## 1. INTRODUCTION

The study of the dynamics of industrial non-Newtonian fluids and their behavior has become more and more popular as many fluids in engineering today exhibit non-Newtonian behavior [1]. Further, the non-Newtonian Bingham plastic fluid flow characteristics are used to show the passage of fluids, specifically fluids for a long time, as well as the development of melts and slurries in moulds [2]. Examining grease speculatively using the Bingham model and returning to Milne [3], he investigated the fundamental 1-D journal and slider bearings and concluded that either surface may have had rigid "cores" added to it. Additionally, a model of the behaviour of Bingham-like fluids that exhibits a yield stress was presented by Dorier and Tichy [2].

Hydrodynamic lubrication is a technique used to reduce friction and wear on fluid-scouring surfaces. Adding the right fluid with the intention that it penetrates the contact area between the scouring surfaces and forms a fluid thin layer is the typical purpose of hydrodynamic lubrication. The majority of the time, this coating reduces friction and wear by keeping the surfaces from coming into contact [4].

Bearings are constantly dependent on incredibly high loads, peak speeds, and severe slip situations. The high load on the treatment in the concentrated contact causes high pressure ageing in the fluid film. For instance, the viscosity of oil varies continuously with pressure and temperature in the high pressure area [5].

In addition, in most of the classical problems lubricant is assumed to be Newtonian. However, since the lubricant is subject to extremely high pressure and shear stresses, as in the case of gear – meshes, heavily loaded rolling element bearings,

which only act for a very short time, the Newtonian behaviour of the lubricant ceases to exist [6]. Besides, many lubricants contain high molecular weight polymers that also make them strongly non-Newtonian [7]. Hence, the effect of non-Newtonian lubricant is to be incorporated along with the effects of pressure and temperature on the lubricants.

On the line of non-Newtonian fluid model, Power law lubricant model has got attention in the recent years because of its simplicity and potential [8]. However, the Bingham plastic model characterizes the flow phenomena of various types of mud and is widely used because of its simplicity, and its capability to determine the loss of pressure in turbulent flow. Also, the Bingham plastic model is the most common rheological model used in the drilling industry. Drilling fluids initially resists flowing. In the Bingham plastic model, the shear stress should exceed a certain value to break the gelation bonding of the drilling fluid and allow it to flow [9].

In the same direction, Kim and Seireg [10] demonstrated the create use of a bi-viscous materials model enforced during a new CFD model to simulate the behavior within the Bingham plastic material in the lubricating film. Jang and Khonsari [11] provided 3-dimensional solutions for the slider bearing lubes with Bingham grease exploitation full thermo-fluid mechanics idea. Prasad et al. [12] analysed thermo-hydrodynamic lubrication options involving uneven rollers lubricated by incompressible power-law fluids supposed for extremely packed rigid line contact system assumptive for the fluid consistency to be modified with pressure and mean film temperature. Further, it had been ended with extended increase of mean temperature with flow behaviour index and rolling ratio. Jang and Khonsari [13] presented overall review on various types of lubrication theory for different Newtonian and

non-Newtonian fluids and their viscosities along with their characteristics. It provided an overall emphasis on the various important characteristics of lubrication theory.

Another hydrodynamic issue involving a rigid system of roller bearings greased with a flimsy compressible fluid for typical squeezing movement was investigated by Prasad et al. [14]. This study concentrated on anticipating that the fluid's consistency and density would vary according to the temperature and pressure. According to Sajja and Prasad's [15] investigation into the role of temperature in the hydrodynamic lubrication of non-Newtonian power-law fluids that are incompressible and intended for highly filled rigid systems, there was a noticeable change in the mean film temperature with flow index and rolling ratio.

Östensen et al. [16] presented a theoretical study on determination of Roelands viscosity and pressure in an elastohydrodynamic rolling contact by using optical interferometry without thermal effects. In the presence of an externally induced magnetic field, Misra and Adhikary [17] examined the steady flow as well as the pulsatile flow of a Bingham plastic fluid. The finite difference method was used to solve the governing equations. On the velocity, volumetric flow rate, and wall shear stress, the impacts of porosity, magnetic field, and yield stress were investigated. In a highly loaded rigid system, Revathi et al. [18] studied non-Newtonian lubrication of asymmetric rollers with incompressible Bingham plastic fluid in rolling/sliding line contact taking into account fluid viscosity variations only with hydrodynamic pressure. The trends in fluid velocity were elaborated, and the results—in particular, the pressure, load, and traction forces—were discovered to be consistent with previous findings. Gadamsetty et al. [19] extended this work and looked into a related issue involving the incompressible Bingham plastic fluid and the lubrication characteristics of anti-symmetric rollers. Results were in good accord with previous findings, especially with regard to temperatures, pressure, traction, and load. A more effective computational lubrication theory for a Bingham plastic fluid was presented by Lampaert and van Ostayen [20]. Since no extra approximations are needed beyond those employed in the generalised Reynolds equation's derivation, the theory is regarded to be precise in this sense. Gadamsetty et al. [21] investigated how an incompressible non-Newtonian Bingham plastic fluid could lubricate a line contact problem for fluid pressure and velocity including temperature.

Not much work has been carried out by the researchers from this field taking into account the asymmetric roller bearings with viscosity as a function of pressure and temperature. Hence in the present work, the attention has been focussed on to analyse such characteristics of bearings lubricated by an incompressible Bingham plastic fluid under cavitation boundary conditions. Roelands viscosity is here considered which is assumed to be a function of pressure and the mean film temperature.

## 2. THEORETICAL MODEL

The system in this study is taken into account in a way that both surfaces have the same radius but are moving at various speeds. Additionally, it is evident that the upper surface is made to move quicker than that of the lower surface. Figure 1 depicts the entire flow configuration.

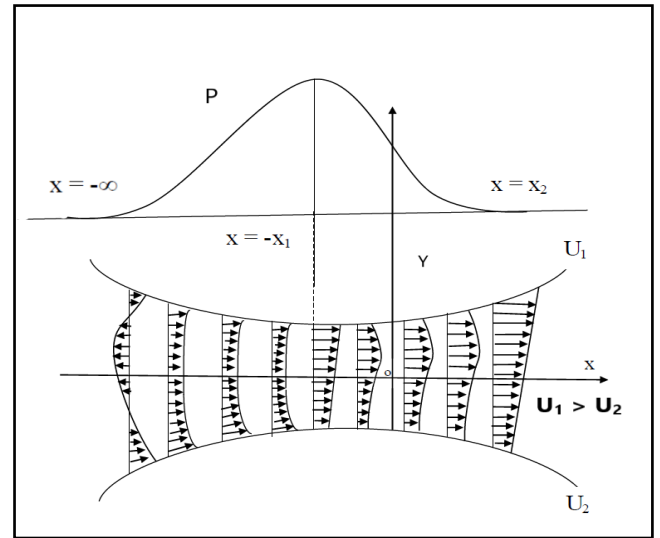


Figure 1. Lubrication of asymmetric rollers

### 2.1 Mathematical formulation

Under common presumptions, the following equations, which regulate the flow of incompressible fluid, are taken into account [19]:

$$\frac{\partial u}{\partial x} + \frac{\partial v}{\partial y} = 0 \quad (1)$$

$$\frac{dp}{dx} = \frac{\partial \tau}{\partial y} \quad (2)$$

where, "p" and "τ" stand for the fluid's hydrodynamic pressure and shear stress, respectively. Sasaki et al. [22] provide the constitutive equation for Bingham plastic fluid.

$$\tau = \pm \tau_0 + \mu \frac{\partial u}{\partial y} \quad (3)$$

where, 'μ' is the Roelands viscosity of the fluid [23] taken by

$$\mu = \mu_0 e^{\left[ \ln(\mu_0) + 9.67 \right] \left[ \left( 1 + \frac{p}{p_r} \right)^z \left( \frac{T_0 - t_0}{T_m - t_0} \right)^{s_0} - 1 \right]} \quad (4)$$

where,  $t_0 = 138^\circ$ , the equation for thickness of the film is to be

$$h = h_0 + \frac{x^2}{2R} \quad (5)$$

'R' represents 'radius of the equivalent cylinder'.

### 2.2 The boundary conditions

The boundary conditions for this problem at both upper and lowers surfaces are taken as

$$u = U_1 \quad \text{at } y = h \quad (6)$$

$$u = U_2 \quad \text{at } y = -h \quad (7)$$

$$p = 0 \quad \text{at } x = -\infty \quad (8)$$

$$p=0 \text{ and } p'(x)=0 \text{ at } x=x_2 \quad (9)$$

where,  $U_1$  and  $U_2$  are the velocities of cylindrical rollers from Figure 1. By utilising the boundary conditions indicated above and solving Eq. (2) as shown below, it is possible to derive the fluid's velocity expression:

$$u = \frac{3}{4h^3}(U_1+U_2)(h-h_1)\left(y^2-h^2\right) + \frac{y}{2h}(U_1-U_2) + \frac{1}{2}(U_1+U_2) \quad (10)$$

$$Q = \int_{-h}^h u dy = h(U_1+U_2) - \frac{2h^3}{3\mu} \frac{dp}{dx} \quad (11)$$

And the 'volume flux' at the point of maximum pressure is

$$Q(-x_1) = (U_1+U_2)h_1 \quad (12)$$

where, the film thickness  $h_1$  at  $x=-x_1$  is regarded to be

$$h_1 = 1 + x_1^2 \quad (13)$$

### 2.3 Reynolds equation

The pressure Reynolds equation is shown below when Eq. (2) is integrated under the boundary conditions (Eqs. (6)-(8)).

$$\frac{dp}{dx} = \frac{3\mu}{2h^3} [(U_1+U_2)(h-h_1)] \quad (14)$$

### 2.4 Dimensionless scheme

In this paper, the following dimensionless approach for roller bearings is used.

$$\begin{aligned} \bar{x} &= \frac{x}{R}, \quad \bar{p} = \frac{p}{p_r}, \quad \bar{\mu}_0 = \frac{RU_2\mu_0}{p_r h_0^2}, \quad \bar{T} = \frac{T}{t_0}, \quad \bar{h} = \frac{h}{h_0}, \quad \bar{y} = \frac{y}{h_0}, \\ \bar{\tau}_0 &= \frac{R\tau_0}{p_r h_0}, \quad \bar{w}_x = \frac{2w_x}{Rp_r}, \quad \bar{w}_y = \frac{2w_y}{Rp_r}, \quad \bar{T}Fh+ = \frac{TFh+}{p_r h_0}, \quad \bar{T}Fh- = \frac{TFh-}{p_r h_0} \\ \bar{\mu} &= \bar{\mu}_0 e^{-\left[ \ln\left(\frac{\bar{\mu}_0 p_r h_0^2}{RU_2}\right) + 9.67 \right] \left[ (1+\bar{p})^{\bar{\tau}_0} \left(\frac{\bar{T}_0-1}{\bar{T}-1}\right)^{80} - 1 \right]} \end{aligned}$$

Using the aforementioned dimensionless technique, the velocity expression and pressure Reynolds equation are presented in dimensionless form.

$$\bar{u} = \left[ \left( \frac{(\bar{h}-\bar{y}) + \bar{U}(\bar{h}+\bar{y})}{2\bar{h}} \right) + \left( \frac{3(\bar{y}^2-\bar{h}^2)(\bar{U}+1)(\bar{h}-\bar{h}_1)}{4\bar{h}^3} \right) \right] \quad (15)$$

$$\frac{d\bar{p}}{d\bar{x}} = \frac{3\bar{\mu}(1+\bar{U})(\bar{h}-\bar{h}_1)}{2\bar{h}^3} \quad (16)$$

### 2.5 Heat equation

To solve the line contact lubrication problem, let's assume the following heat equation [24]

$$\rho c_p \left( u_m \frac{dT_m}{dx} \right) = k \frac{\partial^2 T}{\partial y^2} + \tau \frac{\partial u}{\partial y} \quad (17)$$

The Eq. (3) is used to derive the shear stress ' $\tau$ ' for the Bingham plastic fluid.

The following describe the boundary conditions for the heat equation.

$$T=T_h \text{ at } y=h \text{ and } \frac{\partial T}{\partial y}=0 \text{ at } y=-h \quad (18)$$

The following temperature of the lubricant is obtained by solving for the integral of Eq. (17):

$$T = T_h + \left( \frac{\rho c_p}{2k} \right) \left( u_m \frac{dT_m}{dx} \right) \left( y^2 + 2hy - 3h^2 \right) - \left( \frac{\tau_0}{k} \right) \left[ \left( \frac{U_1-U_2}{4h} \right) \left( y^2 + 2hy - 3h^2 \right) + \left( \frac{U_1+U_2}{4h^3} \right) \left( y^3 - 3h^2y + 2h^3 \right) \right] - \left( \frac{\mu}{k} \right) \left[ \left( \frac{U_1-U_2}{8h^2} \right) \left( y^2 + 2hy - 3h^2 \right) + \left( \frac{3(U_1+U_2)^2(h-h_1)^2}{16h^6} \right) \left( y^4 + 4h^3y - 5h^4 \right) + \left( \frac{(U_1-U_2)(U_1+U_2)(h-h_1)}{4h^4} \right) \left( y^3 - 3h^2y + 2h^3 \right) \right] \quad (19)$$

As a result, the explicit functions of  $x$  and  $y$  for the temperature,  $T$ , are known analytically. The mean temperature is now provided by

$$T_m = \frac{1}{2h} \int_{-h}^h T dy$$

and can be written as:

$$T_m = T_h - \left( \frac{4\rho c_p h^2}{3k} \right) \left( u_m \frac{dT_m}{dx} \right) + \left( \frac{\tau_0}{k} \right) \left[ \left( \frac{2(U_1-U_2)h}{3} \right) - \left( \frac{(U_1+U_2)(h-h_1)}{2} \right) \right] + \left( \frac{\mu}{k} \right) \left[ \left( \frac{(U_1-U_2)^2}{3} \right) + \left( \frac{9(U_1+U_2)^2(h-h_1)^2}{10h^2} \right) - \left( \frac{(U_1-U_2)(U_1+U_2)(h-h_1)}{2h} \right) \right] \quad (20)$$

Now, the dimensionless temperature and mean temperatures are obtained as follows:

$$\bar{T} = \bar{T}_h + \left( \frac{\bar{P}_e}{\bar{P}_e} \right) \left( \bar{u}_m \frac{d\bar{T}_m}{d\bar{x}} \right) \left( \bar{y}^2 + 2\bar{h}\bar{y} - 3\bar{h}^2 \right) - (\bar{P}_R \bar{E}_t) \left[ \bar{\eta} A_1(x) + \bar{\mu} A_2(x) \right] \quad (21)$$

$$\bar{T}_m = \bar{T}_h - \left( \frac{8\bar{h}^2}{3} \bar{P}_e \frac{d\bar{T}_m}{d\bar{x}} \right) + \bar{P}_R \bar{E}_t \left[ \bar{\eta} A_3(x) + \bar{\mu} A_4(x) \right] \quad (22)$$

$$\frac{d\bar{T}_m}{d\bar{x}} = \frac{3}{8\bar{h}^2 \bar{P}_e} \left[ \bar{T}_h - \bar{T}_m + \bar{P}_R \bar{E}_t \left[ \bar{\eta} A_3(x) + \bar{\mu} A_4(x) \right] \right] \quad (23)$$

where,

$$A_1(x) = \left[ \left( \frac{(\bar{U}-1)}{4\bar{h}} \right) \left( \bar{y}^2 + 2\bar{h}\bar{y} - 3\bar{h}^2 \right) + \left( \frac{(\bar{U}+1)(\bar{h}-\bar{h}_1)}{4\bar{h}^3} \right) \left( \bar{y}^3 - 3\bar{h}^2\bar{y} + 2\bar{h}^3 \right) \right]$$

$$A_2(x) = [B_1(x) + B_2(x) + B_3(x)]$$

$$B_1(x) = \left[ \left( \frac{(\bar{U}-1)^2}{8\bar{h}^2} \right) \left( \bar{y}^2 + 2\bar{h}\bar{y} - 3\bar{h}^2 \right) \right]$$

$$B_2(x) = \left( \left( \frac{3(\bar{U}+1)^2(\bar{h}-\bar{h}_1)^2}{16\bar{h}^6} \right) \left( \bar{y}^4 + 4\bar{h}^3\bar{y} - 5\bar{h}^4 \right) \right)$$

$$B_3(x) = \left( \left( \frac{(\bar{U}-1)(\bar{U}+1)(\bar{h}-\bar{h}_1)}{4\bar{h}^4} \right) \left( \bar{y}^3 - 3\bar{h}^2\bar{y} + 2\bar{h}^3 \right) \right)$$

$$A_3(x) = \left[ \left( \frac{2(\bar{U}-1)\bar{h}}{3} \right) - \left( \frac{(\bar{U}+1)(\bar{h}-\bar{h}_1)}{2} \right) \right]$$

$$A_4(x) = \left[ \left( \frac{(\bar{U}-1)^2}{3} \right) + \left( \frac{9(\bar{U}+1)^2(\bar{h}-\bar{h}_1)^2}{10\bar{h}^2} \right) - \left( \frac{(\bar{U}+1)(\bar{U}-1)(\bar{h}-\bar{h}_1)}{2\bar{h}} \right) \right]$$

$$\bar{\gamma} = \frac{p_r U_2 h_0^2}{k R t_0} = \left( \frac{c_p h_0^2 p_r}{K U_2 R} \right) \left( \frac{U_2^2}{t_0 c_p} \right) = \bar{P}_R \cdot \bar{E}_t,$$

$$\bar{p}_e = \frac{\rho c_p u_m h_0^2}{2kR}, \quad \bar{\eta} = \left( \frac{R \tau_0}{h_0 p_r} \right)$$

## 2.6 Load and traction

One of the crucial aspects of loaded bearings is their load capacity, which offers a general idea of the bearings' effectiveness. Therefore, its computation is crucial. The x-component of the load per unit length of the cylinder is given by Sajja and Prasad [15], which is obtained by integrating the pressure throughout the film thickness.

$$W_x = - \int_{-h}^h p dh \quad (24)$$

The non-dimensional load  $\bar{W}$  is given by

$$\bar{W}_x = \int_{-\infty}^{\bar{x}_2} \bar{x}^2 \frac{d\bar{p}}{d\bar{x}} d\bar{x} \quad (25)$$

Similarly, the y-component  $W_y$  of the load is obtained as

$$W_y = \int_{-\infty}^{\bar{x}_2} p dx \quad (26)$$

The non-dimensional load  $\bar{W}_y$  is given by

$$\bar{W}_y = - \int_{-\infty}^{\bar{x}_2} 2\bar{x} \frac{d\bar{p}}{d\bar{x}} d\bar{x} \quad (27)$$

Further, the load components  $W$  is determined by

$$W = \sqrt{W_x^2 + W_y^2} \quad (28)$$

Now, the traction force ' $T_F$ ' at the surfaces can be acquired by solving the shear stress ' $\tau$ ' for the whole length as

$$T_{Fh-} = - \int_{-\infty}^{\bar{x}_2} \tau_{y=-h} dx \quad \text{and} \quad T_{Fh+} = - \int_{-\infty}^{\bar{x}_2} \tau_{y=h} dx \quad (29)$$

Dimensionless tractions are

$$\bar{T}Fh = - \int_{-\infty}^{\bar{x}_2} \left[ \bar{\tau}_0 + \left( \frac{\bar{\mu}}{2h} \right) \left[ (\bar{U}-1) + \frac{3}{h}(\bar{U}+1)(\bar{h}-\bar{h}_1) \right] \right] d\bar{x} \quad (30)$$

$$\bar{T}Fh = - \int_{-\infty}^{\bar{x}_2} \left[ \bar{\tau}_0 + \left( \frac{\bar{\mu}}{2h} \right) \left[ (\bar{U}-1) - \frac{3}{h}(\bar{U}+1)(\bar{h}-\bar{h}_1) \right] \right] d\bar{x} \quad (31)$$

## 3. RESULTS AND DISCUSSION

Numerical computations are performed with the following values in this problem:

$$U_2 = 400 \text{ cm/s}, \quad h_0 = 4 \times 10^{-4} \text{ cm}, \quad R = 3 \text{ cm}, \quad \bar{T}_h = 1.55, \quad t_0 = 1.5,$$

$$p_r = 1.962 \times 10^8, \quad 0 \leq z \leq 0.8, \quad 1 \leq s_0 \leq 1.5$$

### 3.1 Velocity profile

Figures 2-4 calculate and display the fluid's velocity for the regions before, after, and at the point of maximum pressure, respectively. The profiles in the first two graphs have vertices pointing upward and downward in the areas before and after the point of maximum pressure, resembling parabolas.

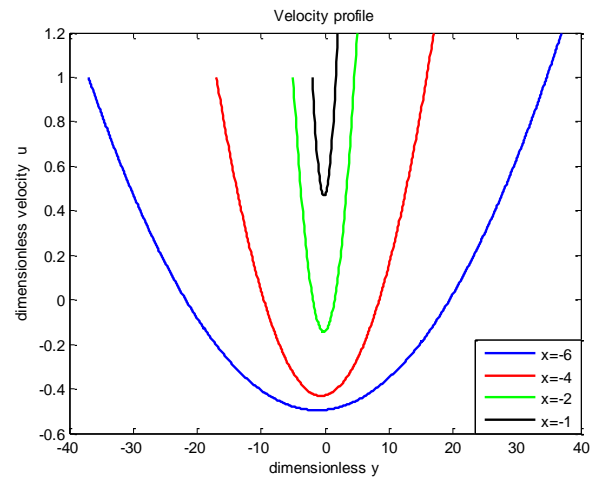


Figure 2. Velocity profile

As seen in Figure 2, the vertices below the  $\bar{y}$  line indicate that there is a reverse flow close to the entrance. Prasad and Subrahmanyam [25] also demonstrated reverse flow. The back flow is eliminated as the fluid moves forward [19, 25]. However, the velocity profile, which can be seen in Figure 4, appears to be increasing linearly at the point of greatest pressure [18].

### 3.2 Pressure profile

For various values of  $\bar{U}$  and  $s_0$ , the pressure distributions  $\bar{p}$  are numerically estimated and shown in Figures 5-6. From Figure 5, it is clear that the hydrodynamic pressure  $\bar{p}$  rises with the rolling-sliding parameter. This suggests that, when compared to a pure rolling example, hydrodynamic pressure is higher for sliding cases. Observations of this type of behaviour were made in [5, 15, 24, 26, 27]. In Figure 6, the lubricating pressure for various values of  $s_0$  the sliding case is shown, and

it is clear that the pressure drops as the value of  $s_0$  increases.

Additionally, the cavitation points for various values of  $\bar{U}$  are estimated numerically and displayed in Table 1. The table shows that as  $\bar{U}$  grows, the cavitation points move further away from the centre line of contact. Physically the pressure region is extended because of high pressure [15]. Same trend is followed in case of points of maximum pressure as  $\bar{x}_1 = \bar{x}_2$ .

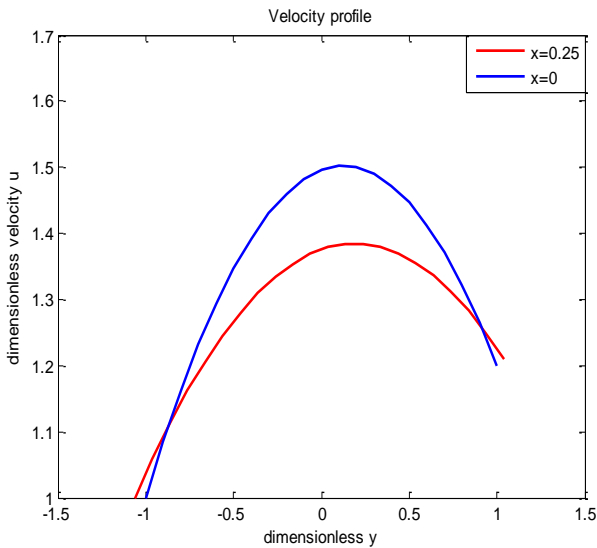


Figure 3. Velocity profile

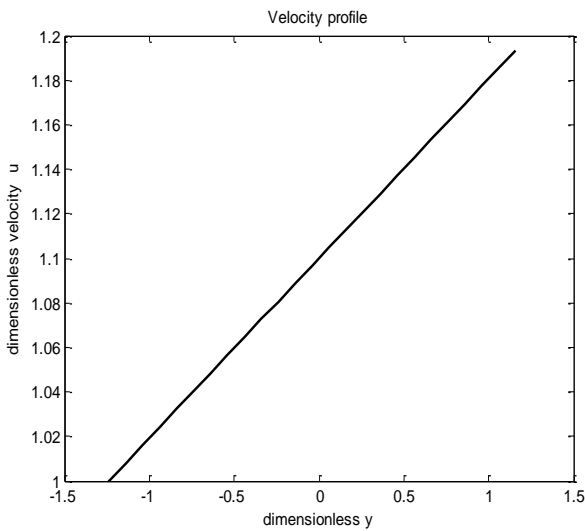


Figure 4. Velocity profile at point of maximum pressure

Table 1. Cavitation points

$U$	$\bar{x}_2$
1.0	0.48982987
1.1	0.48983869
1.2	0.48985873
1.3	0.49026789
1.4	0.49105893
1.5	0.49210927

### 3.3 Viscosity ( $\bar{\mu}$ ) profile

Figures 7-8 show the results for the numerical computation of the lubricant viscosity  $\bar{\mu}$  for various values of  $\bar{U}$  and  $s_0$ .

Figure 7 shows the lubricant viscosity for various values of the rolling-sliding parameter  $\bar{U}$ , and it can be seen that the viscosity reduces as  $\bar{U}$  increases. Additionally, Figure 8 displays the viscosity curve for various values of  $s_0$  and also shows that viscosity reduces with increasing value of  $s_0$ .

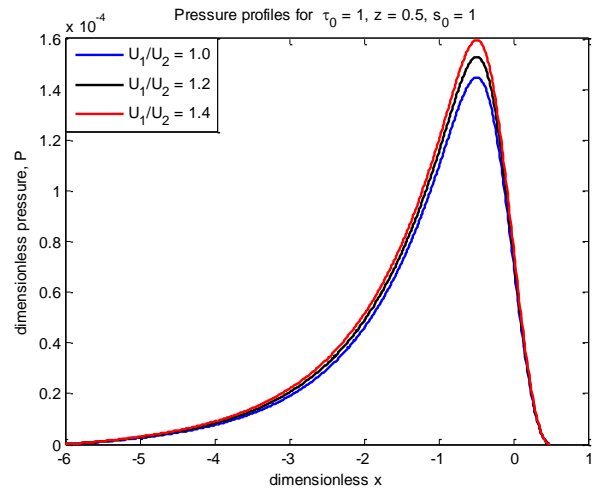


Figure 5. Pressure profile for different  $\bar{U}$

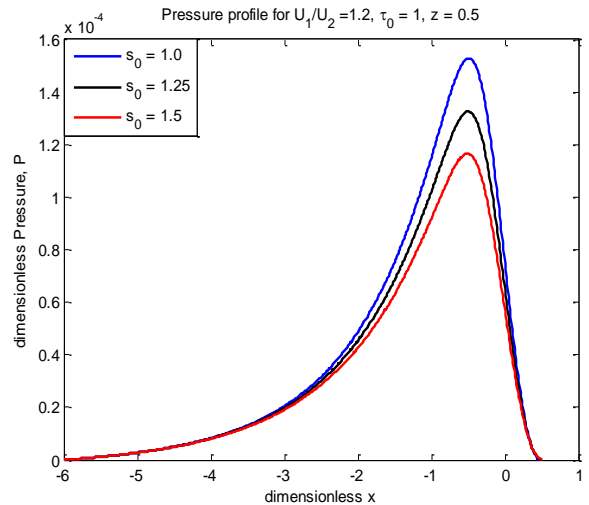


Figure 6. Pressure profile for different  $\bar{U}$

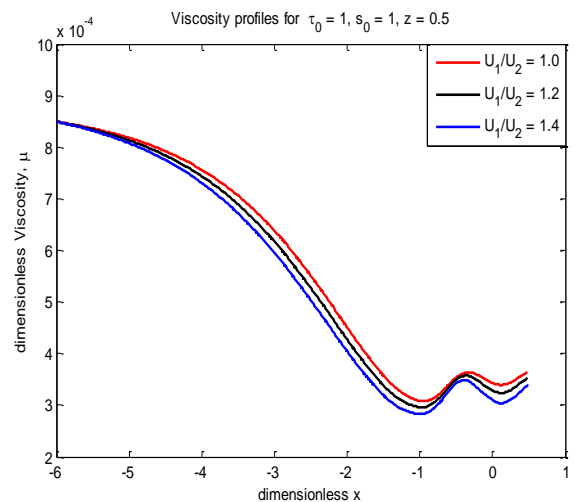


Figure 7. Viscosity profile

### 3.4 Mean temperature profiles

Figures 9-12 elaborate on the dimensionless mean temperature  $\bar{T}_m$  of the lubricant for various values of  $\bar{U}$ ,  $s_0$ ,  $\bar{p}_e$ . In Figure 9, which shows the dimensionless mean temperature profile for various values of  $\bar{U}$  and  $z=0.5$ ,  $s_0=1$ , it can be shown that the mean temperature for the sliding case is larger than that of pure rolling. Lampaert and van Ostayen [20] also noted this type of behaviour. Additionally, it should be noted that the subjective behaviours of  $\bar{T}_m$  versus  $\bar{x}$  are nearly identical to the temperature profiles found for Power-law fluids by Misra, and Adhikary [17] and Prasad and Sajja [25].

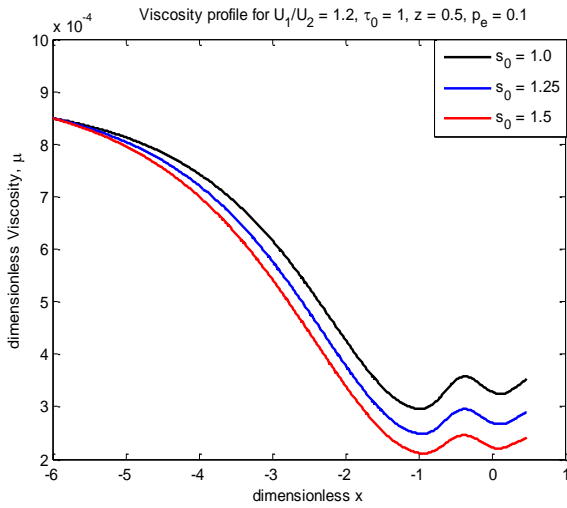


Figure 8. Viscosity profile

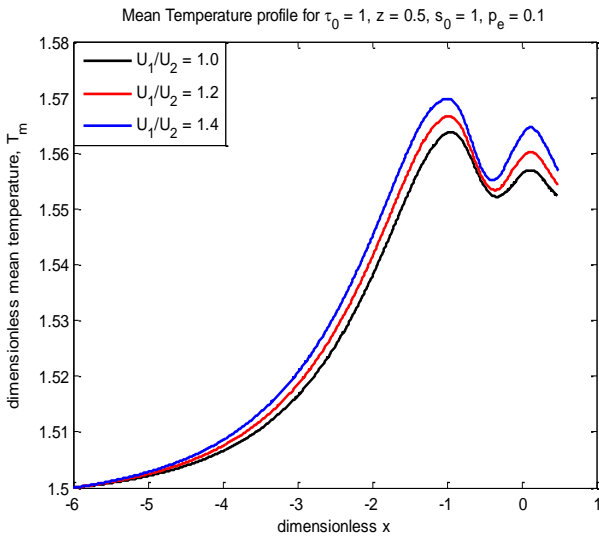


Figure 9. Mean temperature profile

The mean film temperature  $\bar{T}_m$  for different values of  $s_0$ ,  $z=0.5$  and  $\bar{p}_e = 0.1$  is presented in Figures 10-11 for sliding and pure rolling cases respectively. The decrease of mean temperature as  $s_0$  increases in both sliding and pure rolling cases can be observed in both the Figures. The mean temperature  $\bar{T}_m$  for different values of  $\bar{p}_e$  presented in Figure 12 for fixed values of sliding parameter  $\bar{U}=1.2$ ,  $z=0.5$  and  $s_0=1$ . One can see from this Figure 12 that mean temperature

decreases with increase of  $\bar{p}_e$ . Further, in all the temperature profiles,  $\bar{T}_m$  increases throughout the inlet region up to the point of maximum pressure  $\bar{x} = -\bar{x}_1$ , then it decreases up to the origin and thereafter increases after origin and decreases up to the cavitation point  $\bar{x} = \bar{x}_2$ .

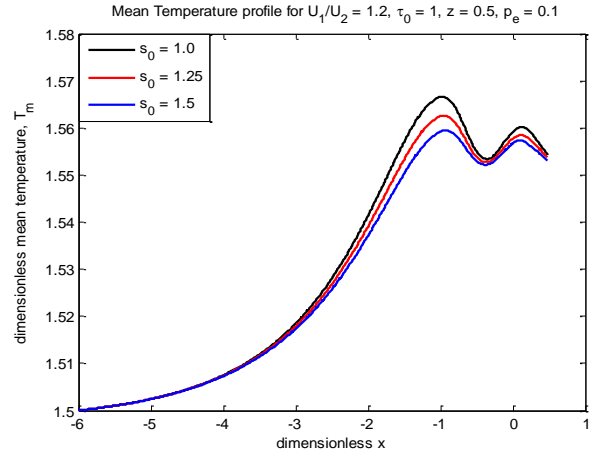


Figure 10. Mean temperature profile

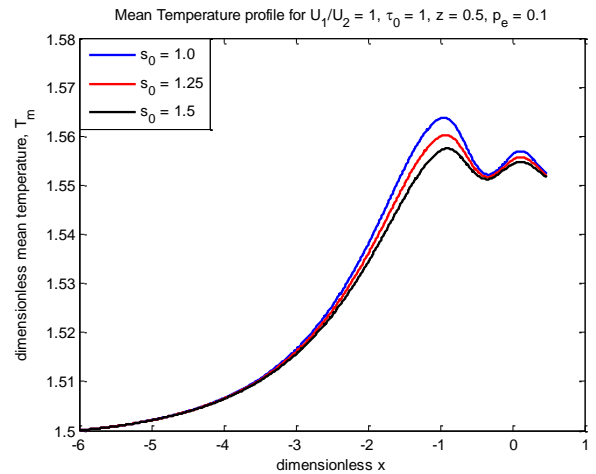


Figure 11. Mean temperature profile

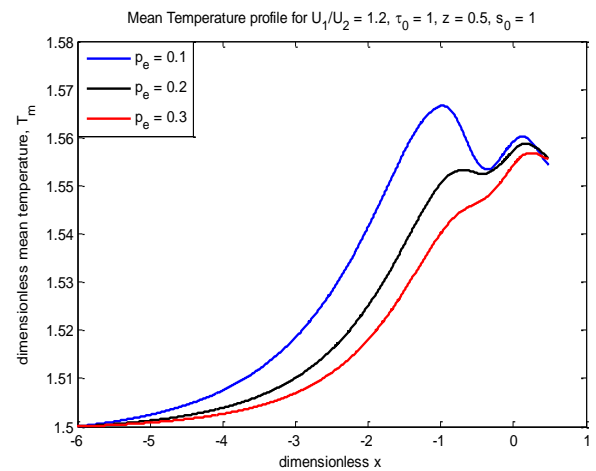


Figure 12. Mean temperature profile

However, an increase or a decrease in  $\bar{T}_m$  beyond the point  $\bar{x} = -\bar{x}_1$  is hardly discernible. The reason for the shape of the

curves in the Figures 9-12 is that, the temperature goes up in inlet region because of dominance of conduction as flow proceeds.

### 3.4 Load and traction

For various rolling ratio  $\bar{U}$  values, the dimensionless load component  $\bar{W}$  is numerically calculated and shown in Table 2. The table demonstrates how load raises rolling ratio. The results obtained by Gadamssetty et al. [19], Gadamssetty et al. [21], and Prasad et al. [27], Prasad et al. [28], and Sajja [24] for the power-law fluid case all agree with the qualitative behaviour of load that was obtained here.

The traction forces  $\bar{T}_{Fh}$  have been computed numerically at both the lower and upper surfaces and presented in Table 3 and Table 4 for distinct values of  $\bar{\tau}_0$  and  $\bar{U}$ . Here  $\bar{\tau}_0=0$  represents Newtonian case and  $\bar{\tau}_0>0$  represents non-Newtonian case. The traction forces increase with  $\bar{\tau}_0$  for fixed value of  $\bar{U}$  at both the lower and upper surfaces. Further, the increase of traction forces with  $\bar{U}$  at upper surface can be observed from Table 4 and indicates that the surface moving with more velocity will have more traction force. These findings are very similar to the results published in Gadamssetty et al. [4], Gadamssetty et al. [21], Prasad et al. [27], Prasad et al. [28], Lubricant Viscosity [23]. Both the surfaces experience the same traction force when they are moving with same velocity.

**Table 2.** Load values

$\bar{U}$	$\bar{W}$
1.0	0.00040544
1.1	0.00041855
1.2	0.00043099
1.3	0.00044261
1.4	0.00045347
1.5	0.00046360

**Table 3.** Traction values at lower surface

$\bar{U}$	$\bar{\tau}_0=0$	$\bar{\tau}_0=0.5$	$\bar{\tau}_0=1$
1.0	0.00060246	2.27728985	4.55395651
1.1	0.00058766	2.27727462	4.55394129
1.2	0.00057326	2.27725983	4.55392649
1.3	0.00055880	2.26057845	4.52057845
1.4	0.00054499	2.26056437	4.52056437
1.5	0.00053181	2.26055095	4.52055095

**Table 4.** Traction values at upper surface

$\bar{U}$	$\bar{\tau}_0=0$	$\bar{\tau}_0=0.5$	$\bar{\tau}_0=1$
1.0	0.00060246	2.27728985	4.55395651
1.1	0.00065904	2.27734683	4.55401350
1.2	0.00071375	2.27740171	4.55406838
1.3	0.00076640	2.26078774	4.52078774
1.4	0.00081648	2.26083763	4.52083763
1.5	0.00086417	2.26088497	4.52088497

### 4. CONCLUSION

With the behaviour of line contact lubricated by an incompressible non-Newtonian Bingham plastic fluid whose viscosity follows the Roelands model; an attempt is made to examine the fluid film lubrication features of rolling and

sliding problem. For various values of  $\bar{\tau}_0$  and the sliding parameter  $\bar{U}$ , the pressure and fluid velocity, continuity and momentum equations are solved. The outcomes of this work can be drawn as follows:

- The velocity of the lubricant is independent of  $\bar{\tau}_0$
- Velocity of the lubricant at point of maximum pressure increases linearly with  $\bar{y}$ .
- The lubricant pressure increases as rolling ratio increases.
- The load component increases with rolling ratio  $\bar{U}$ .
- The traction forces at both the surfaces increase with  $\bar{\tau}_0$ .
- The traction at the upper surface is higher than that of the lower surface due to more speed of upper surface.

**Suggestions:** It can be improved by considering the rollers to be complete asymmetric. That is both surfaces may have different dimensions and moving with different velocities.

### REFERENCES

- [1] Bhattacharyya, K., Banerjee, A., Zaib, A., Mahato, S.K. (2018). MHD mixed convection flow of a non-Newtonian Powell-Eyring fluid over a permeable exponentially shrinking sheet. *Frontiers in Heat and Mass Transfer (FHMT)*, 10(30): 1-8. <http://doi.org/10.5098/hmt.10.30>
- [2] Dorier, C., Tichy, J. (1992). Behavior of a Bingham-like viscous fluid in lubrication flows. *Journal of Non-Newtonian Fluid Mechanics*, 45(3): 291-310. [https://doi.org/10.1016/0377-0257\(92\)80065-6](https://doi.org/10.1016/0377-0257(92)80065-6)
- [3] Milne, A.A. (1954). *Theory of Rheodynamic Lubrication*. *Kolloid Z.*, 139 Haft ½, 96-101.
- [4] Gadamssetty, R., Sajja, V.S., Sudam Sekhar, P., Prasad, D. (2020). Thermal effects in Bingham plastic fluid film lubrication of asymmetric rollers. *Frontiers in Heat and Mass Transfer (FHMT)*, 15(1): 1-7. <http://doi.org/10.5098/hmt.15.18>
- [5] Prasad, D., Subrahmanyam, S.V., Panda, S.S. (2012). Thermal effects in hydrodynamic lubrication of asymmetric rollers using Runge-Kutta-Fehlberg method. *International Journal of Engineering Science & Advanced Technology*, 2(3): 422-437.
- [6] Hirst, W., Moore, A.J. (1978). EHD lubrication of high pressure. *Proceedings of the Royal Society A*, 360: 403-425. <https://doi.org/10.1098/rspa.1978.0076>
- [7] Bourgin, P. (1979). Fluid-film flows of differential fluids of complexity n dimensional approach—applications to lubrication theory. *Journal of Lubrication Technology*, 101(2): 140-144. <https://doi.org/10.1115/1.3453294>
- [8] Sinha, P., Singh, C. (1982). Lubrication of a cylinder on a plane with a non-Newtonian fluid considering cavitation. *ASME, Journal of Lubrication Technology*, 104(2): 168-172. <https://doi.org/10.1115/1.3253176>
- [9] Rehm, B., Haghshenas, A., Paknejad, A.S., Al-Yami, A., Hughes, J. (Eds.). (2013). *Underbalanced drilling: limits and extremes*. Elsevier, Gulf Publishing Company, pp. 39-108. <https://doi.org/10.1016/B978-1-933762-05-0.50009-7>
- [10] Kim, J.H., Seireg, A.A. (2000). Thermohydrodynamic lubrication analysis incorporating Bingham rheological model. *Journal of Tribology*, 122(1): 137-146.

- <https://doi.org/10.1115/1.555336>
- [11] Jang, J.Y., Khonsari, M.M. (2001). On the thermohydrodynamic analysis of a Bingham fluid in slider bearings. *Acta Mechanica*, 148: 165-185. <https://doi.org/10.1007/BF01183676>
- [12] Prasad, D., Panda, S.S., Subrahmanyam, S.V. (2012). Non-Newtonian squeeze film lubrication of journal bearing with temperature effect. *International Journal of Engineering Science & Advanced Technology*, 2(3): 438-444.
- [13] Jang, J.Y., Khonsari, M.M. (2013). Lubrication with a non-newtonian fluid. In: Wang, Q.J., Chung, YW. (eds) *Encyclopedia of Tribology*. Springer, Boston, MA. [https://doi.org/10.1007/978-0-387-92897-5\\_151](https://doi.org/10.1007/978-0-387-92897-5_151)
- [14] Prasad, D., Subrahmanyam, S.V., Panda, S.S. (2014). Thermal, squeezing and compressibility effects in lubrication of asymmetric rollers. *Tribology in Industry*, 36(3): 244-258.
- [15] Sajja, V.S., Prasad, D. (2015). Characterization of lubrication of asymmetric rollers including thermal effects. *Industrial Lubrication and Tribology*, 67(3): 246-255. <https://doi.org/10.1108/ILT-04-2013-0048>
- [16] Östensen, J.O., Larsson, R., Venner, C.H. (1996). Determination of viscosity and pressure in an elastohydrodynamic rolling contact by using optical interferometry: A theoretical study. *Proceedings of the Institution of Mechanical Engineers, Part J: Journal of Engineering Tribology*, 210(4): 259-268. [https://doi.org/10.1243/PIME\\_PROC\\_1996\\_210\\_507\\_0\\_2](https://doi.org/10.1243/PIME_PROC_1996_210_507_0_2)
- [17] Misra, J.C., Adhikary, S.D. (2017). Flow of a Bingham fluid in a porous bed under the action of a magnetic field: Application to magneto-hemorheology. *Engineering Science and Technology, an International Journal*, 20(3): 973-981. <https://doi.org/10.1016/j.jestch.2016.11.008>
- [18] Revathi, G., Sajja, V.S., Prasad, D. (2019). Bingham plastic fluid film lubrication of asymmetric rollers. *International Journal of Scientific and Technology Research*, 8(11): 2549-2554.
- [19] Gadamsetty, R., Sajja, V., Lanka, S., Prasad, D. (2020). Thermohydrodynamic lubrication of asymmetric rollers by Bingham plastic fluid. *Solid State Technology*, 63(5): 6165-6181.
- [20] Lampaert, S.G., van Ostayen, R.A. (2020). Lubrication theory for Bingham plastics. *Tribology International*, 147: 106160. <https://doi.org/10.1016/j.triboint.2020.106160>
- [21] Gadamsetty, R., Sajja, V.S., Sudam Sekhar, P., Prasad, D. (2021). Squeeze film lubrication of asymmetric rollers by Bingham plastic fluid. *Frontiers in Heat and Mass Transfer (FHMT)*, 16(7): 1-6. <http://dx.doi.org/10.5098/hmt.16.7>
- [22] Sasaki, T., Mori, H., Okino, N. (1962). Fluid lubrication theory of roller bearing—Part I: Fluid lubrication theory for two rotating cylinders in contact. *Journal of Basic Engineering*, 84(1): 166-174. <https://doi.org/10.1115/1.3657240>
- [23] Lubricant Viscosity. [https://www.tribonet.org/wiki/lubricant-viscosity/?utm\\_source=tribonet+community&utm\\_campaign=f923444c2c-EMAIL\\_CAMPAIGN\\_2017\\_12\\_03\\_COPY\\_02&utm\\_medium=email&utm\\_term=0\\_79f2001725-f923444c2c-215516733](https://www.tribonet.org/wiki/lubricant-viscosity/?utm_source=tribonet+community&utm_campaign=f923444c2c-EMAIL_CAMPAIGN_2017_12_03_COPY_02&utm_medium=email&utm_term=0_79f2001725-f923444c2c-215516733), accessed on 07<sup>th</sup> November, 2021.
- [24] Sajja, V.S. (2016). Thermal effects in non-Newtonian lubrication of asymmetric rollers under adiabatic and isothermal boundaries. *International Journal of Chemical Sciences*, 14(3): 1641-1656.
- [25] Prasad, D., Sajja, V.S. (2016). Non-Newtonian lubrication of asymmetric rollers with thermal and inertia effects. *Tribology Transactions*, 59(5): 818-830. <https://doi.org/10.1080/10402004.2015.1107927>
- [26] Revathi, G., Sajja, V.S., Prasad, D. (2019). Thermal effects in power-law fluid film lubrication of rolling/sliding line contact. *International Journal of Innovative Technology and Exploring Engineering*, 8(9): 277-283. <http://doi.org/10.35940/ijitee.H7195.078919>
- [27] Prasad, D., Singh, P., Sinha, P. (1988). Nonuniform temperature in non-Newtonian compressible fluid film lubrication of rollers. *Journal of Tribology*, 110(4): 653-658. <https://doi.org/10.1115/1.3261708>
- [28] Prasad, D., Shukla, J.B., Singh, P., Sinha, P., Chhabra, R.P. (1991). Thermal effects in lubrication of asymmetrical rollers. *Tribology International*, 24(4): 239-246. [https://doi.org/10.1016/0301-679X\(91\)90050-J](https://doi.org/10.1016/0301-679X(91)90050-J)

## NOMENCLATURE

$\overline{E}_t$	Eckert number
h	Film thickness
h <sub>0</sub>	Minimum film thickness
p	Hydrodynamic pressure
$\frac{P_e}{P_R}$	Peclet number
$\frac{P_R}{P_R}$	Prandtl number
T <sub>Fh</sub>	Traction force
u	Fluid velocity in x-direction
v	Fluid velocity in y-direction
$\overline{x}_1$	Point of maximum pressure
$\overline{x}_2$	Point of cavitation
U <sub>1</sub> , U <sub>2</sub>	Velocities of the surfaces

## Greek symbols

μ	Viscosity of the lubricant
μ <sub>0</sub>	Coefficient of viscosity
τ	Shear stress
τ <sub>0</sub>	Yield stress
ρ	Density of the lubricant